Journal of Polymer Research (2022) 29: 27
https://doi.org/10.1007/s10965-021-02831-4

ORIGINAL PAPER

Core–shell structure flame retardant Salen-PZN-Cu@Ni-Mof microspheres enhancing fire safety of epoxy resin through the synergistic effect

Tingxiang He[1] · Junhong Guo[1] · Chengxia Qi[1] · Rui feng[2] · Baoping Yang[1] · Yingping Zhou[1] · Li Tian[1] · Jinfeng Cui[1]

Received: 21 April 2021 / Accepted: 10 November 2021 / Published online: 28 December 2021

Abstract

Phosphorus-containing organic–inorganic hybrid flame retardant with core–shell structure (Salen-PZN-Cu@Ni-Mof) was prepared. Thermogravimetric analysis (TGA) showed that when the additive amount was only 3wt%, the introduction of Salen-PZN-Cu@Ni-Mof significantly improved the thermal stability of epoxy resin (EP) composites. The results of the cone calorimeter test showed that adding 3wt% Salen-PZN-Cu@Ni-Mof made the peak of heat release rate (PHRR), total heat release (THR), smoke production rate (SPR) and total smoke production (TSP) of epoxy resin composites reduced by 30.4%, 10.8%, 29.5% and 6.8%, respectively. It was proved that Salen-PZN-Cu@Ni-Mof could significantly enhance the fire safety of epoxy resin composites, which was attributed to the synergetic combination of the flame retardant effect of the phosphazene structure itself, the catalyzed carbon formation of various metal ions and the porous mof materials with strong adsorption properties. Besides, it was found that the Ni-Mof could strengthen the compatibility between the flame retardant and the EP matrix effectively through the tensile test. The novel core–shell structure flame retardant Salen-PZN-Cu@Ni-Mof promised to be a functional filler that integrated features of flame retardancy and high ductility.

Keywords EP composites · Flame retardant mechanism · Fire safety · Smoke suppression · Synergistic effect

Introduction

With the development of synthetic materials, flame retardants are developing all the time. It is of great significance to developing a polymer flame retardant for polymer materials which can achieve long-term and high efficiency attribute to the compound flame retardants have a good flame retardant effect and flexible structure is easy to be chemically modified [1, 2].

Since the twenty-first century, the halogen flame retardants are limited by the release of corrosive hydrogen halide gas and toxic smoke when burned, which will not only pollute the environment, corrode equipment, but also seriously threaten people's Safety [3]. In addition, a large number of flame retardants will reduce the mechanical properties of the polymer matrix. Therefore, it is necessary to develop new flame retardants which are environmentally friendly, high-efficiency, high-processability and long-lasting flame retardants. Generally speaking, flame retardants for polymer have a strong chemical modification, long-term flame retardancy and great structural flexibility. It is of great significance to develop new polymer flame retardants to achieve long-term high-efficiency flame retardancy.

Polyphosphazene (PZN), a kind of popular hybrid organic–inorganic materials with much excellent performances, has good flame retardancy due to the active phosphazene unit (–P=N–) on the main chain and the structural diversity of the side chain groups for physical or chemical modification is of great flexibility. For this reason, polyphosphazene has a wide range of applications due to its excellent high thermal stability and structural diversity, such as biological materials [4], optical materials [5, 6], electrical materials [7, 8], membrane materials [9, 10] and hybrid materials [11, 12] and so on. Typically,

✉ Junhong Guo
guojh@lut.edu.cn

✉ Li Tian
tianli04@163.com

[1] School of Petrochemical Technology, Lanzhou University of Technology, Pengjiaping Road 36, Lanzhou 730050, China

[2] Polypropylene Project Preparation Company, Huating Coal Corporation, Dongyi Road 3, Huating 744103, China

polyphosphazenes have been applied as flame-retardant additives, which consisted of linear polyphosphazenes, cyclophosphazene units and all of these polyphosphazene-containing materials show higher limiting oxygen index (LOI) values and improve the flame retardancy of the polymer matrix. However, the low yield and high cost of linear polyphosphazenes limit their application. Cyclophosphazene, the other polyphosphazenes, exhibiting good flame retardancy and self-extinction, is widely used to prepare nano- or micro-scale polymers through polycondensation reaction. Significant progress has been made in the research of cross-linked polyphosphazene materials. The design and preparation of new PZNs materials have been widely concerned by many researchers and become research focus on flame retardant. Flame retardants containing metal compounds have excellent catalytic activity and are commonly used in the flame retardant field [13–16]. Qiu et al. [17] introduced three-dimensional nanostructure PZM@Co2P@RGO based on cobalt phosphide, heteroatom-doped mesoporous carbon spheres and graphene into EP. The addition of PZM@Co2P@RGO markedly reduced the fire hazard of EP, such as the maximum peak heat release rate decreased by 47.9% and the total heat release rate decreased by 29.2%, the releasing amount of the toxic gas CO reduced and a higher graphitized protective carbon layer formed. The improvement of the flame retardancy for the composite is attributed to the synergy of P, Co and RGO in PZM@Co2P@RGO.

Schiff base is a class of organic compounds obtained by the dehydration condensation reaction of amine and aldehyde compound, containing functional imine group $R_1R_2C=NR_3$. The reaction has the advantages of a simple process, conditions that are easy to control and high yield. Schiff base compounds can be complexed with metal ion M^{n+} Salen ligand is a chelating Schiff base formed by condensation polymerization of two aldehyde molecules and one diamine molecule. Due to its simple preparation, low cost and diversified structure, it has been widely used in the fields of biotechnology [18, 19], photoelectric functional materials [20, 21], medical treatment [22, 23], corrosion resistance materials [24, 25], analytical chemistry, and so on [26, 27]. Ramgobin et al. [28]. studied Salen-based flame retardants of different metal ions and evaluated the flame retardant effect of thermoplastic polyurethane, finding that different Salen-metal could induce different decomposition pathways when mixed with TPU, its heat release rate (HRR) and total heat release rate (THR) reduced compared with pure TPU, proving that Salen-Metal material can give TPU excellent flame retardancy.

Metal organic framework materials (Mofs) are a kind of organic–inorganic hybrid materials formed by complex reactions between organic ligands and inorganic components (metal ions or clusters). Organic–inorganic hybrid materials have not only good compatibility with the polymer matrix, but also high thermal stability and structural adjustability. They are often used to improve the flame retardancy and mechanical properties of polymers. At present, many types of metal organic framework materials have been synthesized and most of these with high porosity has excellent chemical stability. Mofs are widely used in CO_2 adsorption [29, 30], gas separation [31], magnetic materials [32] and catalysts [33]. Researchers have found that mofs have a wide range of application prospects in the field of flame retardant, more and more researches focus on mofs as flame retardant in recent years. Hou et al. [34] regarded mofs as a flame retardant applied in polymer materials, and they added Co-Mof and Fe-Mof prepared with a facile solvothermal method into polystyrene (PS) and found that adding mofs can improve thermal stability and flame retardancy of PS composites significantly. Compared with pure PS, the peak heat release rates of PS/Fe-Mof and PS/Co-Mof reduced by more than 14% and 28%, respectively, which would provide a potential application in the growth of fire safety for polymer materials.

In this paper, a new multifunctional organic–inorganic hybrid flame retardant Salen-PZN-Cu@Ni-Mof microspheres with core–shell structure were synthesized successfully and its microscopic morphology and structure were characterized and analyzed. Then the flame retardant (Salen-PZN-Cu@Ni-Mof) was added into the EP matrix to study its effect and mechanism of flame retardancy and smoke suppression.

Experimental

Materials

2, 4-Dihydroxybenzaldehyde (DHBD) and o-Phenylendiamine (OPLD) were purchased from Aladdin Industrial Corporation. Ethanol and triethylamine (TEA) were acquired from Tianjin Fuyu Fine Chemical Co. Ltd. (China). Hexachlorocyclotriphosphazene (HCCP), Copper(II) acetate monohydrate and p-Phthalic acid (PTA) were purchased from Aladdin Industrial Corporation. Nickel (II) chloride hexahydrate was supplied by Sinopharm Chemical Reagent Co., Ltd. (Shanghai, China). The epoxy resin (DGEBA, E-44, EEW-227) was purchased from Jiangsu Sanmu Chemical Co., Ltd. (China). N, N-Dimethylformamide (DMF) was purchased from Guangdong Guanghua Sci-Tech Co., Ltd. (China). 4,4'-diaminodiphenyl methane (DDM) was purchased from Shanghai Energy Chemical Co., Ltd, China.

Synthesis of salen-Cu basis polyphosphazenes microspheres (Salen-PZN-Cu)

The synthesis process of core–shell flame retardant Salen-PZN-Cu@Ni-Mof is shown in Scheme 1.

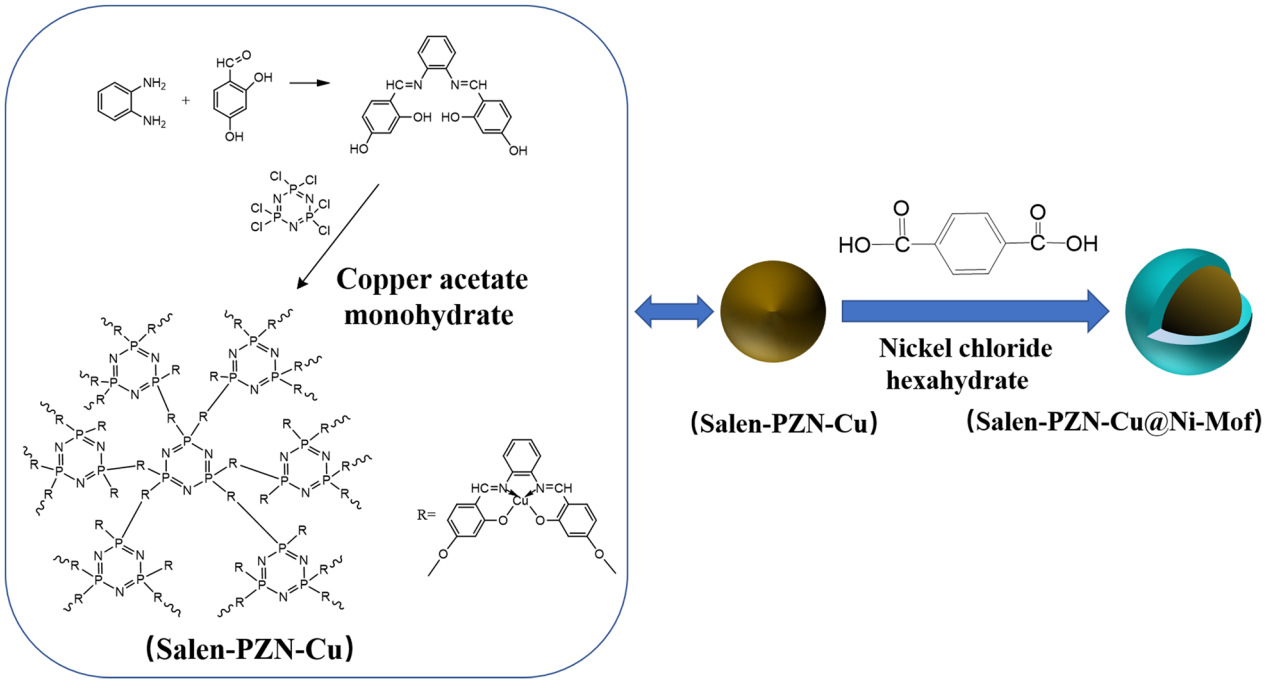

Scheme 1 Synthesis route of core–shell flame retardant Salen-PZN-Cu@Ni-Mof

First of all, Salen-PZN was synthesized based on an earlier report [35]. DHBD(10 g, 71 mmol) and OPLD(3.86 g, 36 mmol)were added into a 500 mL round-bottom flask with 300 mL ethanol as solvent. The reaction was carried out at room temperature for 6 h under magnetic stirring. After the reaction was completed, the obtained yellow solid was filtered, washed with ethanol three times, and then the filter residue dried in a vacuum oven at 60 °C for 12 h to obtain Salen-H6.

Salen-H6 (0.40 g,1.15 mmol) and acetonitrile were added into a 500 mL round-bottom flask with ultrasonic treatment for 30 min. After the salen-H6 powder was dispersed entirely in the acetonitrile, 80 mL of TEA was added into the solutions mentioned above stirring magnetically for 1 h. At this time, the mixture turned into a clear and transparent solution with orange-yellow color. Then HCCP (0.04 g, 0.16 mmol) was added into acetonitrile dropwise for 1 h. Then stirring for 4 h until the reaction process completed, the filtered sediment was washed with water and ethanol, respectively for three times to get rid of impurity, and then the filter residue dried in a vacuum oven at 60 °C for 12 h to obtain Salen-PZN powder(0.35 g).

Next, 1.02 g Salen-PZN powder was added into 50 mL DMF solution reacting with 1.17 g Copper(II) acetate monohydrate for 4 h. The filtered sediment was washed with water and ethanol respectively to remove impurity and then the filter residue dried in a vacuum oven at 60 °C for 12 h to obtain Salen-PZN-Cu powder(1.41 g).

Synthesis of Ni-Mof

PTA (0.12 g,0.75 mmol) was added in a mixed solvent containing DMF(32 mL), ethanol (2 mL) and deionized water(2 mL), Nickel (II) chloride hexahydrate (0.18 g,0.75 mmol) and 0.8 mL TEA were added with stirring and ultrasonic treatment. After reacting 8 h, the filtered sediment was washed with water and ethanol, respectively three times and then the filter residue dried in a vacuum oven at 60 °C for 12 h to obtain Ni-Mof (0.22 g).

Synthesis of Salen-Cu basis polyphosphazenes @ Ni-Mof Microspheres (Salen-PZN-Cu@Ni-Mof)

PTA (0.12 g, 0.75 mmol) was added in a mixed solvent containing DMF(32 mL), ethanol (2 mL) and deionized water(2 mL). Salen-PZN-Cu(0.6 g) was dispersed completely into the mixture mentioned above with ultrasonic treatment for 1 h, Nickel(II) chloride hexahydrate (0.18 g,0.75 mmol) and 0.8 mL TEA were added. After reacting 8 h, the filtered sediment was washed with water and ethanol, respectively three times and then the filter residue dried in a vacuum oven at 60 °C for 12 h to obtain Salen-PZN-Cu@Ni-Mof (0.76 g).

Synthesis of EP/ Salen-PZN-Cu@Ni-Mof and EP/ Ni-Mof

3wt% Salen-PZN-Cu@Ni-Mof/EP was prepared using the method of solution blending. 60 g EP was stirred mechanically in the container at 110 °C for 1 h to reduce its stickiness and 2.32 g Salen-PZN-Cu@Ni-Mof was added under high-speed agitation. Then 15.15 g of DDM was added under continuous stirring until the DDM was completely dissolved and the molten mixed solution was quickly poured into preheated PTFE plate mold for solidification. The curing procedures were set in order at 120 °C for 2 h, 140 °C for 2 h,160 °C for 2 h successively to obtain EP composites. Pure EP samples are prepared in the same way as EP composites. The preparation method of EP/Ni-MOF is the same as above.

Characterization

Fourier transform infrared (FTIR) spectra were tested in the range of 4000–400 cm^{-1} on an FTIR-850 Spectrometer (TianJin GangDong Sci. & Tech. Development Co., Ltd, China). KBr was blended with the sample powder and pressed into tablets for analysis.

Scanning electron microscopy (SEM) was conducted on a JSM-5600 LV scanning electron microscope to analyze the surface morphology and structure of samples and carbon residue of EP composites after the cone calorimeter test.

Transmission electron microscopy (TEM) was tested on a JEM-2100F (Japan Electron Optics Laboratory Co., Ltd., Japan).

The spectra of X-ray photoelectron spectroscopy (XPS) were received from ESCALAB 250Xi X-ray photoelectron spectrometer to explore the chemical elements of the sample.

Thermogravimetric analysis (TGA) of the samples and EP composites was conducted to explore thermal stability on HCT-1 instrument (Beijing Henven Scientific Instrument Factory, China) at a heating rate of 10 °C/min under air and nitrogen atmosphere.

The combustion behavior of EP and EP composites was characterized by a cone calorimeter (FTT, UK) at a heating flux of 50 kW/m^2. The dimension of samples was $100 \times 100 \times 3mm^3$.

Laser Raman Spectroscopy (LRS) was tested on HORIBA Scientific, France, in the range from 800 to 2000 cm^{-1} at room temperature to explore the structure, components and graphitization degree of the residual char.

The tensile strength of EP composites was tested on the electronic universal testing machine (Jinan hengruijin testing machine Co., Ltd, China), and the corresponding samples size was $130 \times 10 \times 4mm^3$.

Results and discussion

Characterization of Ni-Mof, Salen-PZN-Cu and Salen-PZN-Cu@Ni-Mof

Figure 1 presents the SEM images of Ni-Mof (a), Salen-PZN-Cu (b, c), Salen-PZN-Cu@Ni-Mof (d, e) and TEM images of Salen-PZN-Cu (f, g) and Salen-PZN-Cu@Ni-Mof (h, i), respectively, giving the microstructure and morphology of flame retardant. It can be seen from Fig. 1a that the Ni-Mof is layer-packed. From Fig. 1b, c, it was found that Salen-PZN-Cu microspheres exhibit a uniform sphere shape with a rough surface and its average diameter is about 1 μm. Figure 1d, e are composite fire retardant Salen-PZN-Cu@Ni-Mof in different magnification. It can be observed obviously that the layer-packed Ni-Mof is coated on the rough surface of the Salen-PZN-Cu microspheres and the diameter of the Salen-PZN-Cu microspheres coated with Ni-Mof was 1 ~ 2 μm. Figure 1f–i are TEM images of Salen-PZN-Cu and Salen-PZN-Cu@Ni-Mof. It can also be seen that layer-packed mof covered the Salen-PZN-Cu microspheres, which confirmed that Salen-PZN-Cu@Ni-Mof microspheres with core–shell structure were successfully synthesized.

Figure 2 shows the infrared spectrum analysis results of Ni-Mof (black), Salen- PZN-Cu (red) and Salen-PZN-Cu@Ni-Mof (blue). 1587 cm^{-1}, 1355 cm^{-1} is the antisymmetric stretching vibration and symmetric stretching vibration of O-C = O group, 3604 cm^{-1} and 3344 cm^{-1} are -OH stretching vibration, 1240 cm^{-1} is stretching vibration of P = N group; 1590 cm^{-1} corresponds to the peak of the P-Ph group, 1106 cm^{-1} and 998 cm^{-1} are the stretching vibrations of the PO-Ar group. In summary, Salen-PZN-Cu@Ni-Mof microspheres are successfully synthesized.

XPS is used for analyzing the component elements of the specimen. Figure 3 is the XPS survey spectra results of Ni-Mof, Salen-PZN-Cu and Salen-PZN-Cu@Ni-Mof. It can be seen from the spectrum that N, Ni and Cu elements all appeared on the surface of Salen-PZN-Cu@Ni-Mof, illustrating that layered Ni-Mof successfully covers the rough surface of the Salen-PZN-Cu microsphere and Salen-PZN-Cu@Ni-Mof is successfully prepared.

TG characterization

Thermogravimetric analysis is used to explore the thermal oxidation behavior of Ni-Mof, Salen-PZN-Cu and Salen-PZN-Cu@Ni-Mof under air and the thermal degradation behavior under a nitrogen atmosphere, respectively. The TGA curves are shown in Fig. 4. It can be seen from the figure that the thermal degradation pathway of

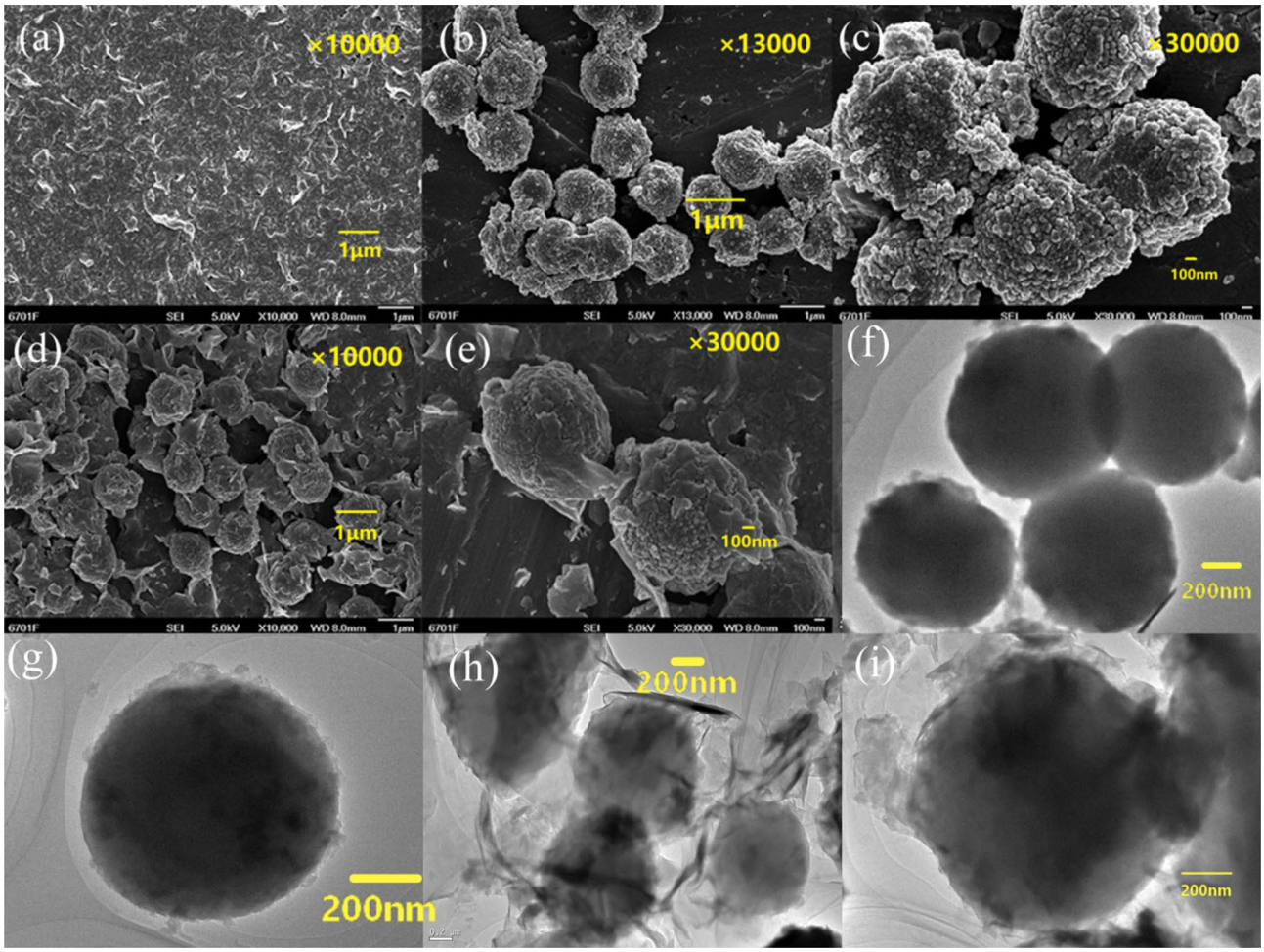

Fig. 1 SEM images of Ni-Mof (**a**),Salen-PZN-Cu (**b**, **c**), Salen-PZN-Cu @Ni-Mof (**d**, **e**) and TEM images of Salen-PZN-Cu (**f**, **g**), Salen-PZN-Cu@Ni-Mof (**h**, **i**)

Ni-Mof under air is the same as under a nitrogen atmosphere, with almost no difference. $T_{5\%}$ is used to describe the temperature at which the sample loses 5% in weight. When Ni-Mof degrades under air or nitrogen, its $T_{5\%}$ and residual carbon are almost identical, namely 132 °C or 135 °C, 22.67% or 23.59%, indicating that Ni-Mof is not inclined to form metal oxides at high temperatures and has good thermal stability. The degradation process of Salen-PZN-Cu is divided into two steps under air, In comparison, Salen-PZN-Cu@Ni-Mof degrades in three stages, indicating that the introduction of Ni-Mof exactly affects the degradation mechanism of flame retardant. The introduction of Ni-Mof makes the $T_{5\%}$ (117 °C) of the composite flame retardant higher than that of Salen-PZN-Cu significantly, and the carbon residue (22.67%) is also higher than that of Salen-PZN-Cu (8.35%) after thermal decomposition. It was proved that Ni-Mof and Salen-PZN-Cu in Salen-PZN-Cu@Ni-Mof synergistically improve the thermal stability of the composite flame retardant. Under a nitrogen atmosphere, Salen-PZN-Cu has the same thermal degradation process as Salen-PZN-Cu@Ni-Mof, and the mass tends to increase slightly at around 650 °C, showing that some chemical reaction on phosphazene may occur. Moreover, $T_{5\%}$ (156 °C) and residual carbon (72.81%) of the composite flame retardant are higher than $T_{5\%}$ (91 °C) and residual carbon (69.24%) of Salen-PZN-Cu with the introduction of Ni-Mof, which illustrates Ni-Mof and Salen-PZN-Cu have synergistic effects on improving the thermal stability of flame retardant.

Characterization of EP and EP composites

Thermal stability of EP composites

The thermal stability of EP and EP composites has been analyzed using TGA and DTG. The results are shown in Figs. 5 and 6. The degradation route of EP and EP

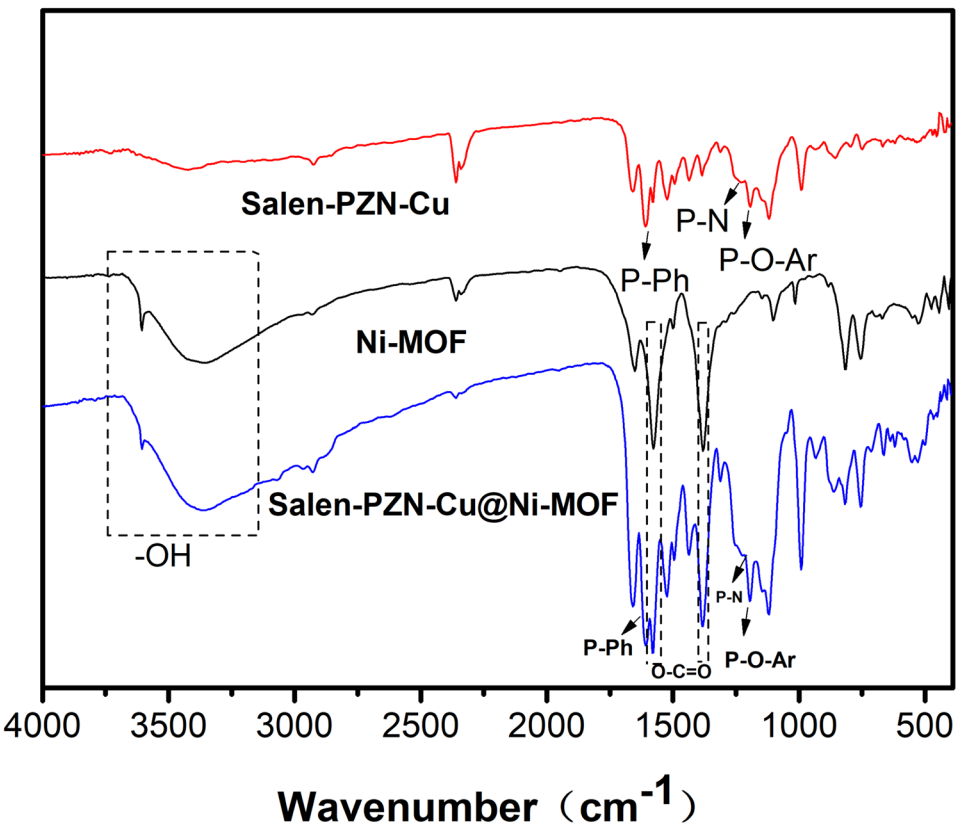

Fig. 2 FTIR spectra of Ni-Mof, Salen-PZN-Cu and Salen-PZN-Cu@Ni-Mof

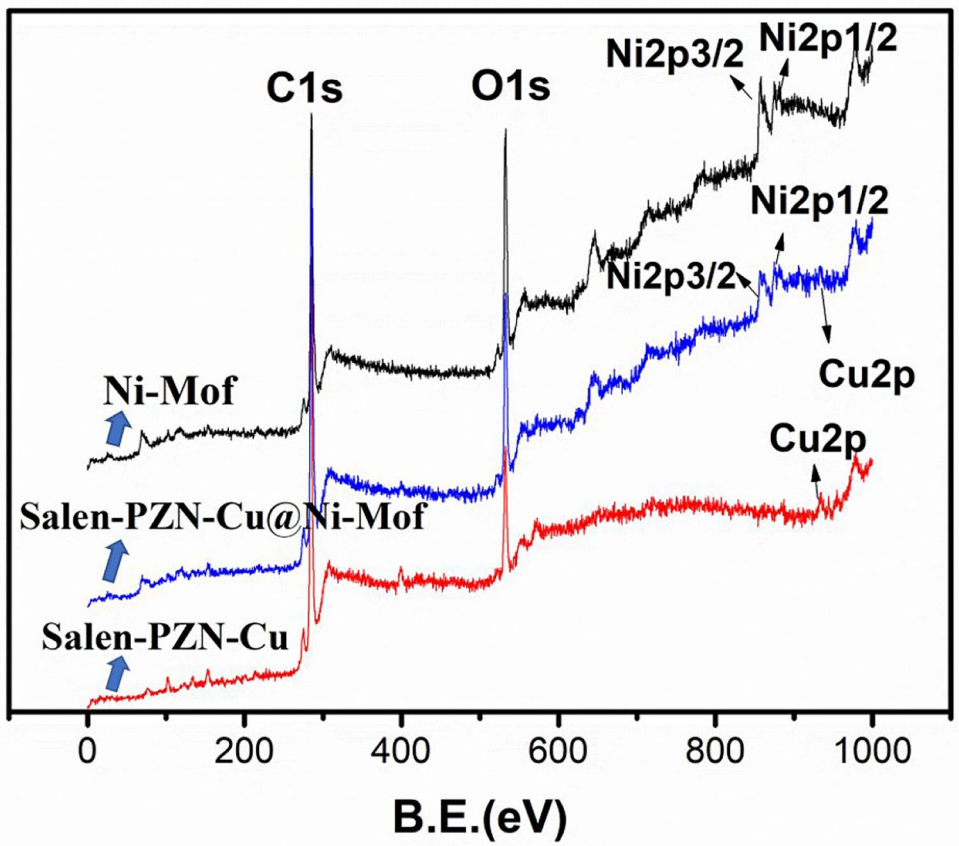

Fig. 3 XPS spectrum of Ni-Mof, Salen-PZN-Cu and Salen-PZN-Cu@Ni-Mof

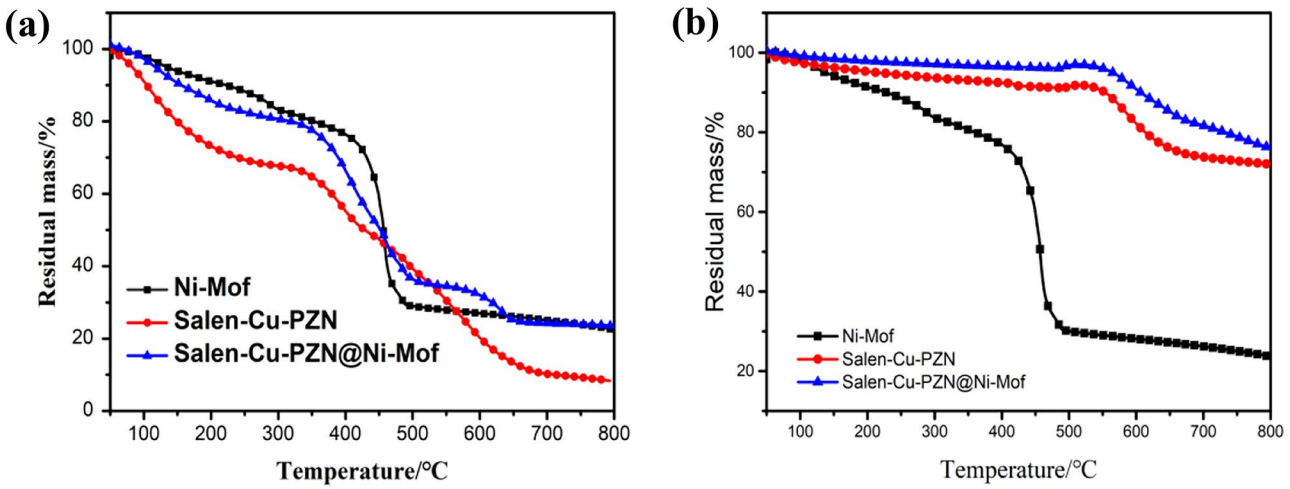

Fig. 4 TG curves of Ni-Mof, Salen-PZN-Cu and Salen-PZN-Cu @ Ni-Mof under air(**a**) and nitrogen atmosphere (**b**)

composites can be divided into two steps under an air atmosphere. When the additive amount is 3wt%, its first degradation stage is at 350 ~ 450 °C, whose weight loss rate is faster, and the peak of maximum weight loss rate appears at about 380 °C, At the same time, all materials just show a single degradation stage under nitrogen atmosphere and the temperature range is also at 350 ~ 450 °C, indicating that the degradation behaviors under two atmosphere are similar to a certain(between 350 ~ 450 °C). The secondary degradation of polymer materials in the air occurs in the range from 500 °C to 750 °C. The carbon layer produced by the first thermal degradation has poor thermal stability and the secondary oxidation reaction occurs. With the temperature increasing, oxygen is involved in the reaction, and some stable products remain in the residue. After the secondary degradation, the residual carbon loses weight again, and a broad weight loss peak appears. In contrast, the weight loss rate of EP composites that have been degraded is slower and tends to be gentle in nitrogen. The initial degradation temperature ($T_{5\%}$) of epoxy resin with the addition of Ni-Mof, Salen-PZN-Cu, or composite core–shell flame retardant Salen- PZN-Cu@Ni-Mof reduces, due to the catalysis action of metal ions, causing EP composites to decompose in advance[28]. However, $T_{5\%}$ of 5wt% Salen-PZN-Cu@Ni-Mof/EP doesn't decrease anymore and

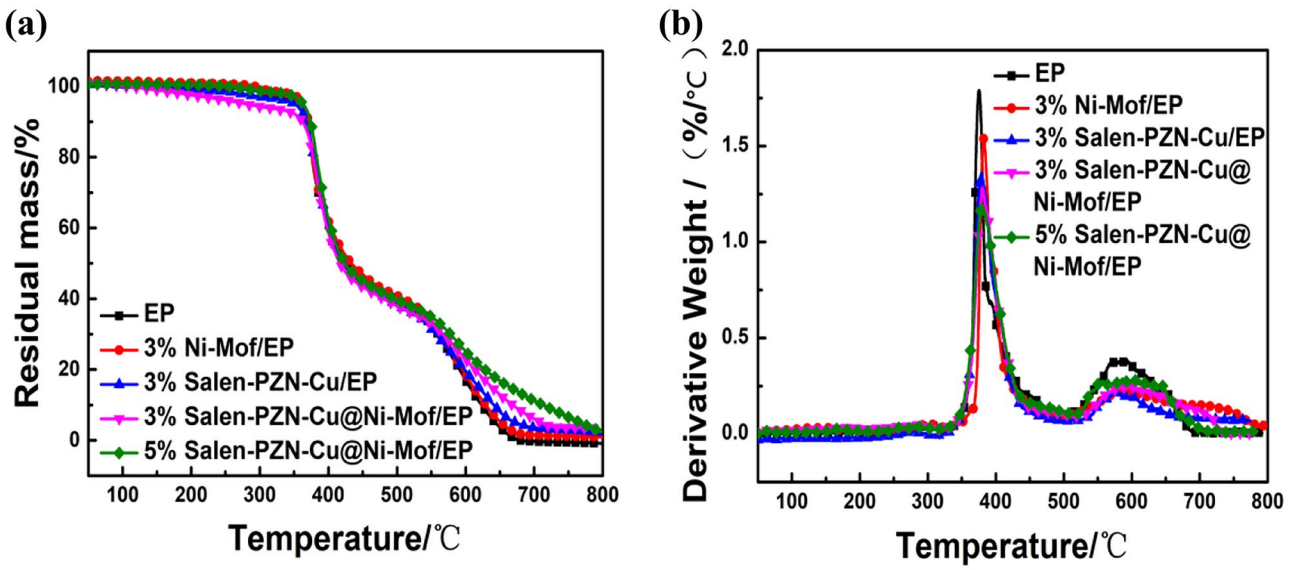

Fig. 5 TG (**a**) and DTG (**b**) curves of Ni-Mof, Salen-PZN-Cu and Salen-PZN-Cu@Ni-Mof under air atmosphere

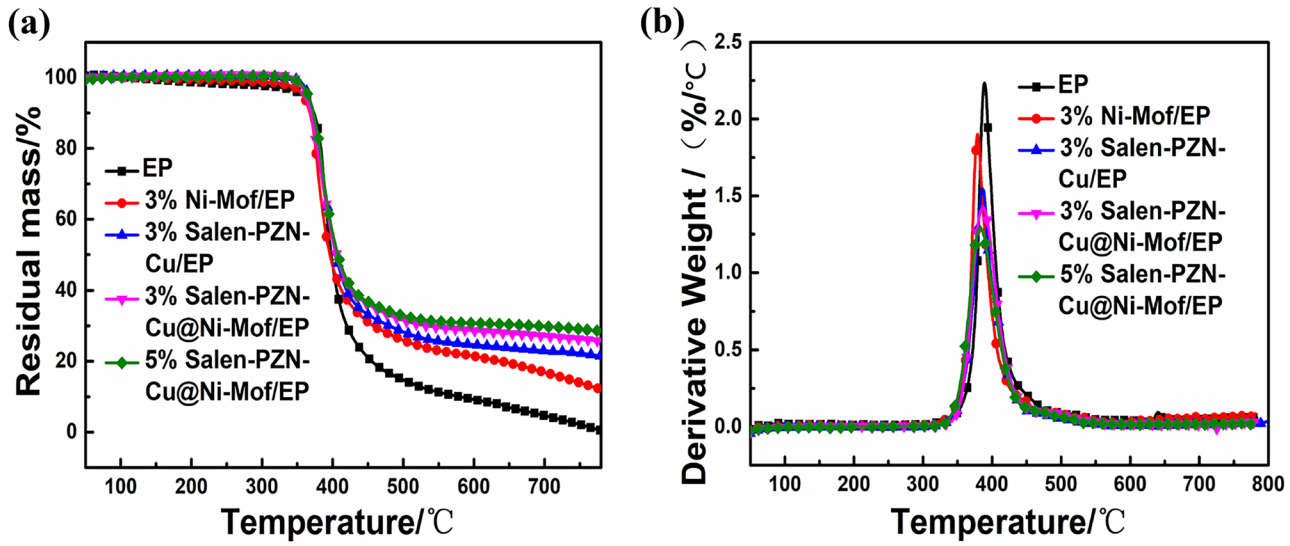

Fig. 6 TG (**a**) and DTG (**b**) curves of Ni-Mof、Salen-PZN-Cu and Salen-PZN-Cu @ Ni-Mof under nitrogen atmosphere

has the highest carbon residue, because a more enormous amount of Salen-PZN-Cu@Ni-Mof works. Moreover, the carbon residue of EP composites increases compared with that of pure EP. The carbon residue is formed by burning polymer acts as a protective layer and protects the polymer from heat and flame, which slows the heat release rate of the material effectively. Whether in the air or nitrogen, the residual carbon content of EP with introducing Salen-PZN-Cu@Ni-Mof is higher than that of the only equivalent amount of Ni-Mof or Salen-PZN-Cu,which indicates that both Ni-Mof and Salen-PZN-Cu influence the thermal stability of EP, and they can synergically improve the thermal stability of EP composites when the addition amount is 3wt%. DTG curves also illustrate this point: The addition of Ni-Mof, Salen- PZN-Cu and Salen-PZN-Cu@Ni-Mof significantly reduced the maximum weight loss rate of the polymer, and EP added Salen-PZN-Cu@Ni-Mof has a lower weight loss rate than Ni-Mof, Salen-PZN-Cu, proving that Ni-Mof and Salen-PZN-Cu in composites flame retardant have a synergistic effect on strengthening the thermal stability.

Flame retardancy of neat EP and EP composites

The cone calorimeter test (CC) is usually used to simulate the real fire scene which the results are closely related to those of large-scale combustion tests to analyze the performance of flame retardants, providing important references in materials evaluation and designing, that is of great significance in the application of flame retardant materials.

The heat release rate (HRR), total heat release (THR), smoke production rate (SPR), total smoke production (TSP), CO release and total CO curves for EP and EP composites obtained from the cone calorimeter test are shown in Fig. 7 and Table 3. The peak heat release rate (PHRR) of EP composites was reduced by 19.6% and total heat release (THR) decreased by 7.4% after introducing 3wt% Ni-Mof into EP. It was proved that Ni-Mof prevented EP matrix effectively from releasing heat and played particular a certain role on flame retardant, which metal oxides and metal carbonates are formed on the surface of the polymer when it burned to catalyze the formation of the carbon layer and protective barrier effectively between the condensed phase and the flame to restrain further burning [36]. Furthermore, it can be seen from Table 3 that Ni-Mof reduce the total release of CO apparently, this is because Mof as a porous material, characterized by larger pore volume and greater specific surface area, has good adsorption performance, it absorbs the toxic fumes released by burning polymer materials and improve the smoke suppression property of polymers [37]. When 3wt% Salen-PZN-Cu was added, PHRR, THR and SPR of EP composites were reduced by 23.7%,9.3%,29.4%, respectively. The reason behind this is that phosphorus components produced polyphosphate at high temperature causing dehydration and carbonization, which inhibits the continuous combustion of the material and plays an active role on fire safety, while CO release was not improved clearly. When 3wt% Salen-PZN-Cu@Ni-Mof is added, the PHRR, THR, SPR and TSP of EP composites decreased by 30.4%, 10.8%, 29.5% and 6.8%, respectively, which are all higher than those of equivalent amount of Ni-Mof or Salen-PZN-Cu. It was shown that

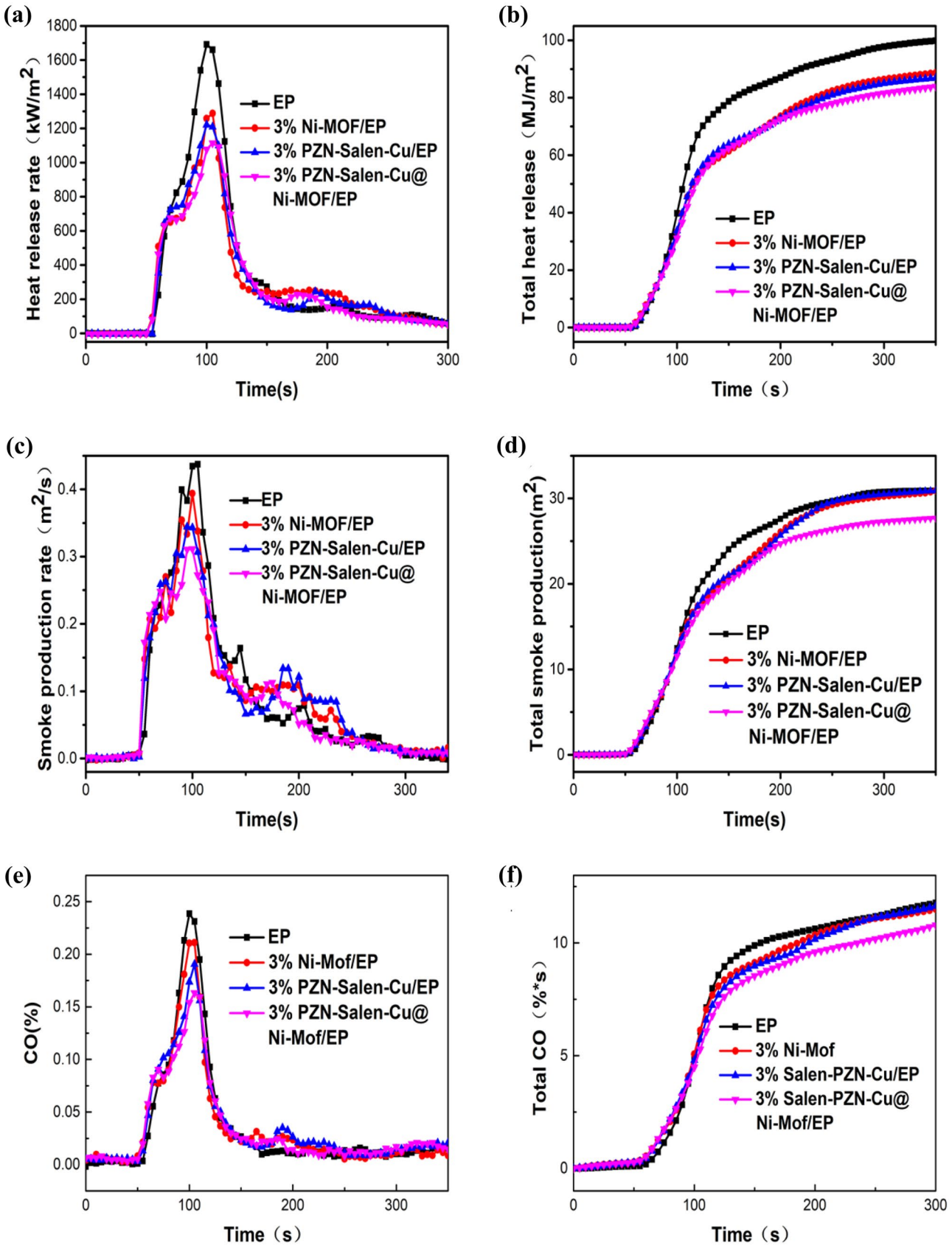

Fig. 7 HRR (**a**), THR (**b**), SPR (**c**), TSP (**d**), CO (**e**) and Total CO (**f**) curves of Ni-Mof、Salen-PZN-Cu and Salen-PZN-Cu @ Ni-Mof under air

Ni-Mof and Salen-PZN-Cu have a synergistic effect on enhancing the thermal stability of flame retardant. That is Ni-Mof makes up for the shortcoming of flame retardancy in the gas phase for Salen-PZN-Cu meanwhile enhances the flame retardancy of Ni-Mof in condensation phase. Meanwhile, under the catalysis of multiple metal ions, the carbon layer, as a physical barrier, becomes denser and prevents the volatile degradation products from escaping, conducive to fire safety. Time to ignition (TTi) also illustrates this point: TTI of the EP with the addition of 3wt% flame retardant Salen-PZN-Cu@Ni-Mof with core–shell structure is shorter than the addition of the same content of Ni-Mof or Salen-PZN-Cu.

Table 1 TG data of EP and EP composites under air atmosphere

Sample	$T_{5\%}$ (°C)	T_{max1} (°C)	T_{max2} (°C)	Char yield(800 °C,%)
EP	369.8	376.6	582.9	0.52
3% Ni-Mof/EP	365.5	383.2	579.2	0.91
3% Salen-PZN-Cu/EP	357.7	380.4	621.4	2.1
3% Salen-PZN-Cu@Ni-Mof/EP	355.9	372.5	598.6	2.57
5% Salen-PZN-Cu@Ni-Mof/EP	354.8	377.5	607.5	3.55

Table 2 TG data of EP and EP composites under nitrogen atmosphere

Sample	$T_{5\%}$ (°C)	T_{max} (°C)	Char yield (800 °C,%)
EP	370.0	389.8	1.5
3% Ni-Mof/EP	355.9	378.5	11.9
3% Salen-PZN-Cu/EP	369.8	388.1	21.7
3% Salen-PZN-Cu@Ni-Mof/EP	365.1	386.9	25.9
5% Salen-PZN-Cu@Ni-Mof/EP	362.3	381.3	28.6

Char residue analysis

SEM analysis of char residue

SEM was used to analyze the surface morphology of carbon residue of Salen-PZN-Cu/EP and Salen-PZN-Cu@Ni-Mof/EP after cone calorimeter test with the magnification of 200x (a, b) and 500x (c) and the images are shown in Fig. 8. It was showed that the carbon residue structure of EP with only 3wt% Salen-PZN-Cu is loose and porous, and the pore size is larger, because the phosphazene structure in PZN generates non-inflammable gases such as N_2, water vapor at high temperature during decomposition of EP, When the equal amount of Salen-PZN-Cu@Ni-Mof is added, some changes in carbon residue structure of EP composites are observed: The carbon residue surface swells, producing a membrane that bulges like bubbles, and the pore size reduced, making the carbon residue surface more compact and continuous, it shows that Ni-Mof has a flame retardant effect on EP and this effect is not only reflected in the gas phase, but also the solidification phase. Moreover, Ni ions can catalyze the formation of carbon layers. In addition, there are many unsaturated metal sites in Mof materials enhancing catalytic activity, promoting the dehydration and carbonization of the EP and protecting the polymer from heat and flame during combustion to achieve the aim of flame retardancy.

LRS analysis of char residue

Laser Raman Spectroscopy is used to investigate the structure of carbon residue graphitization degree. Laser Raman spectra obtained from scattering at 1585 cm^{-1} (G band) and (D band) 1350 cm^{-1} exhibits two characteristic peak, the strength of G band is closely related to the ideal graphite lattice, while D band is related to the disordered graphite structure. The intensity ratio ID/IG of D band and G band is applied to describe the degree of graphitization of carbon residue. The lower the ID/IG value, the higher graphitization degree of carbon residue, the better the morphology, and the fewer lattice defects. The

Table 3 Combustion data from cone calorimeter of EP and EP composites

Sample	PHRR (KW/m^2)	THR (MJ/m^2)	SPR (m^2/s^{-1})	TSP (m^2)	Total CO(%*s)	TTI (s)
EP	**1601.0**	**106.65**	**0.44**	**30.94**	**17.89**	**54**
3% Ni-Mof/EP	**1287.7**	**98.74**	**0.39**	**31.18**	**14.83**	**53**
3% Salen-PZN-Cu/EP	**1220.8**	**96.74**	**0.34**	**31.99**	**18.99**	**53**
3% Salen-PZN-Cu@Ni-Mof/EP	**1114.2**	**95.17**	**0.31**	**28.84**	**17.25**	**51**

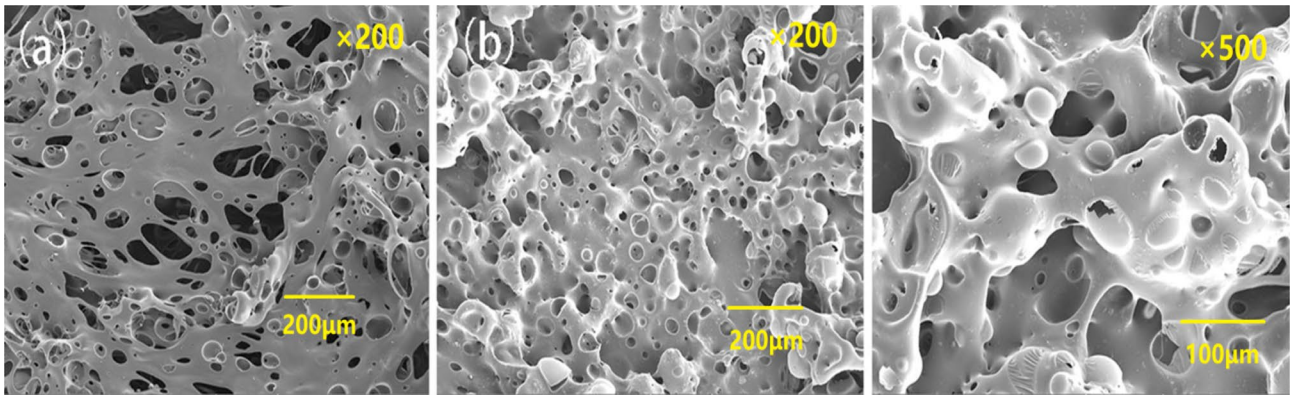

Fig. 8 SEM images of char residue of Salen-PZN-Cu/EP (**a**) and Salen-PZN-Cu@Ni-Mof/EP (**b**, **c**)

structure of carbon residue is analyzed by Laser Raman spectroscopy, and the results are shown in Fig. 9. The ID/IG value of char residue for pure EP is 2.29. It decreases by 14% after the introduction of Salen-PZN-Cu@Ni-Mof into EP. It was proved that Salen-PZN-Cu@Ni-Mof can effectively promote EP carbonization under fire, enhance the continuity and density of the carbon layer structure after burning, which shows the flame retardant effect is consistent with SEM results.

XPS analysis of char residue

C1s, O1s, N1s, P2p, Cu2p and Ni2p spectra for carbon residue of EP and EP composites are analyzed and compared according to Fig. 10a. It was find that P2p and Cu2p signal peaks appear with the introduction of the core–shell flame retardant Salen-PZN-Cu@Ni-Mof, indicating that P, Ni and Cu elements all participate in the process of carbonization to promote the formation of carbon residue and improve the flame-retardant efficiency for the condensed phase. The fine structure of the various elements is further explored through XPS-peak-differentiation-imitating analysis and the element peak spectra of carbon residue for EP and EP composite are shown in Fig. 10b–h. Peaks at 284.7 eV, 285.9 eV, 286.3 eV and 288.3 eV correspond to C–C/H, C-N, C-O and C = O, respectively and peaks at 532.1 eV, 533.6 eV, 534.3 eV correspond to C–O–C, O-C, O–H; peaks at 132.6 eV and 133.2 eV correspond to P–C and P = O bond, indicating phosphate structure exists in the carbon residue. Peaks at 855.7 eV and 860 eV peaks correspond to Ni-C and Ni–O bonds and peaks at 934.3 eV, 941.2 eV and 943.7 eV

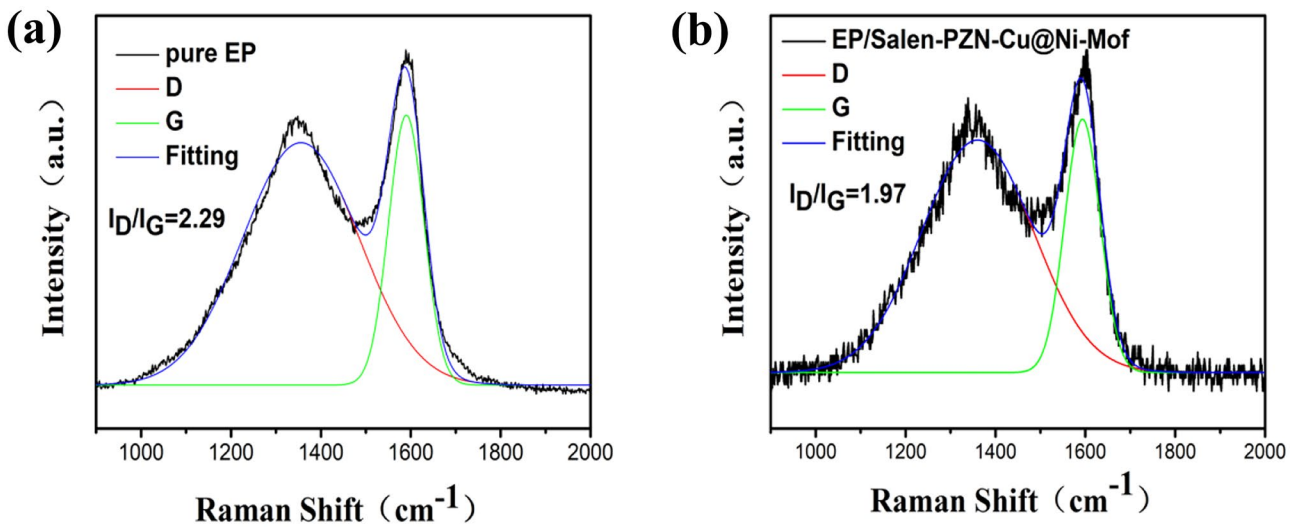

Fig. 9 Laser Raman spectra of char residue of EP and Salen-PZN-Cu@Ni-Mof/EP

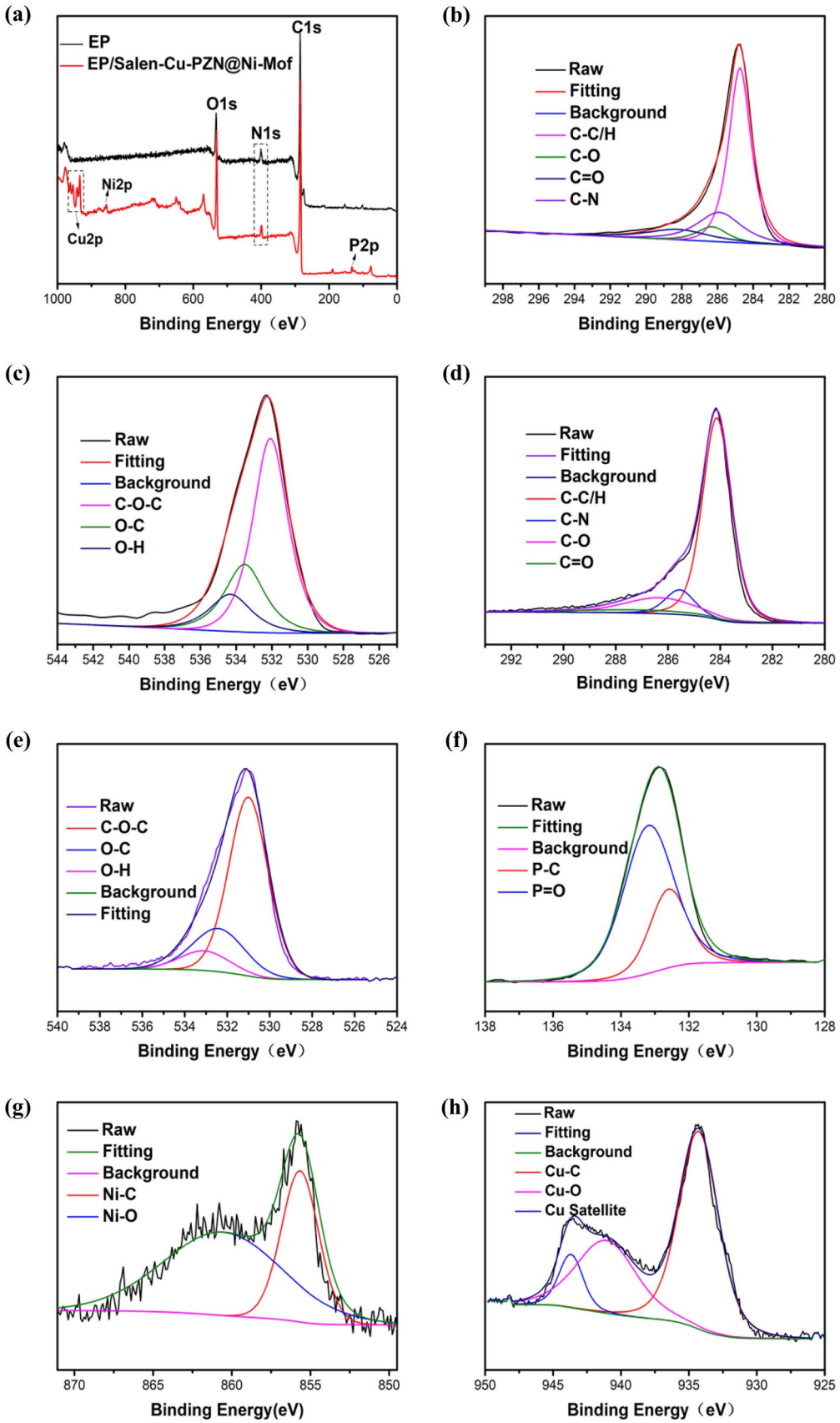
(a)
EP
EP/Salen-Cu-PZN@Ni-Mof
C1s
O1s
N1s
Ni2p
Cu2p
P2p
1000 800 600 400 200 0
Binding Energy（eV）
(b)
Raw
Fitting
Background
C-C/H
C-O
C=O
C-N
298 296 294 292 290 288 286 284 282 280
Binding Energy(eV)
(c)
Raw
Fitting
Background
C-O-C
O-C
O-H
544 542 540 538 536 534 532 530 528 526
Binding Energy（eV）
(d)
Raw
Fitting
Background
C-C/H
C-N
C-O
C=O
292 290 288 286 284 282 280
Binding Energy(eV)
(e)
Raw
C-O-C
O-C
O-H
Background
Fitting
540 538 536 534 532 530 528 526 524
Binding Energy（eV）
(f)
Raw
Fitting
Background
P-C
P=O
138 136 134 132 130 128
Binding Energy（eV）
(g)
Raw
Fitting
Background
Ni-C
Ni-O
870 865 860 855 850
Binding Energy(eV)
(h)
Raw
Fitting
Background
Cu-C
Cu-O
Cu Satellite
950 945 940 935 930 925
Binding Energy（eV）

◂**Fig. 10** XPS spectra for char residue of pure EP and Salen-PZN-Cu@Ni-Mof/EP (**a**); C1s and O1s spectra for char residue of EP(**b**, **c**);C1s,O1s,P2p,Ni2p,Cu2p spectra for char residue of Salen-PZN-Cu@Ni-Mof/EP (**d**–**h**)

correspond to Cu-C bond, Cu–O bond and the satellite peak of Cu, which shows that both Ni and Cu react with oxygen to form nickel oxide and copper oxide at high temperature.

Mechanical properties of EP composites

The mechanical properties of EP and EP composites are investigated by an electronic universal testing machine. The results of pure EP and EP composites are shown in Fig. 11 and Table 4. It can be seen from the figure that the addition of flame retardant reduces Young's modulus signify the rigidity of the pure EP. Compared with 3wt% Salen-PZN-Cu/EP, the elongation at break of Salen-PZN-Cu@Ni-Mof / EP with the same amount increased by 42.6%. It proves that Ni-Mof improves the compatibility of Salen-PZN-Cu/EP effectively, based on the larger contact area between flame retardant and matrix was formed, intermolecular interaction force was enhanced, and the flame retardant is uniformly dispersed in the epoxy resin. Moreover, Young's modulus increases by 13.8% to demonstrate the introduction of Ni-Mof can improve the toughness of EP composites and make the material hard to fracture. When 5wt% Salen-PZN-Cu@Ni-Mof is added into EP, Young's modulus and elongation at break of EP composites compared with 3wt% Salen-PZN-Cu@Ni-Mof /EP decreased 16.37% and 7.32%, respectively. This is because too many additives damage the compatibility between flame retardant and EP matrix, and degrade the mechanical properties of EP composites. The Salen-PZN-Cu@Ni-Mof microsphere coated with Ni-Mof has a core–shell microsphere structure that presents specific morphology, has some impact on toughening for thermosetting resin. The novel flame retardant Salen-PZN-Cu@Ni-Mof is expected to be a functional filler with advantages of flame retardancy and toughening.

Mechanism of flame retardancy and smoke suppression

Based on the above discussion, we can infer that the introduction of Salen-PZN-Cu@Ni-Mof can effectively improve the fire safety of the EP and its flame-retardant mechanism acts on the condensed phase and the gas phase. When EP is decomposed, Salen-PZN-Cu releases free radicals of PO, PO_2, HPO_2, etc., produce non-combustible gas such as N_2 and water vapor to play a role in flame retardance in the gas phase [38]. Salen is a chelating Schiff base with characteristic group (–C = N–), previous researches showed that it undergoes polycondensation through covalent cross-linking at high temperatures to form a cross-linked network structure, which is similar to phenolic resin, playing flame

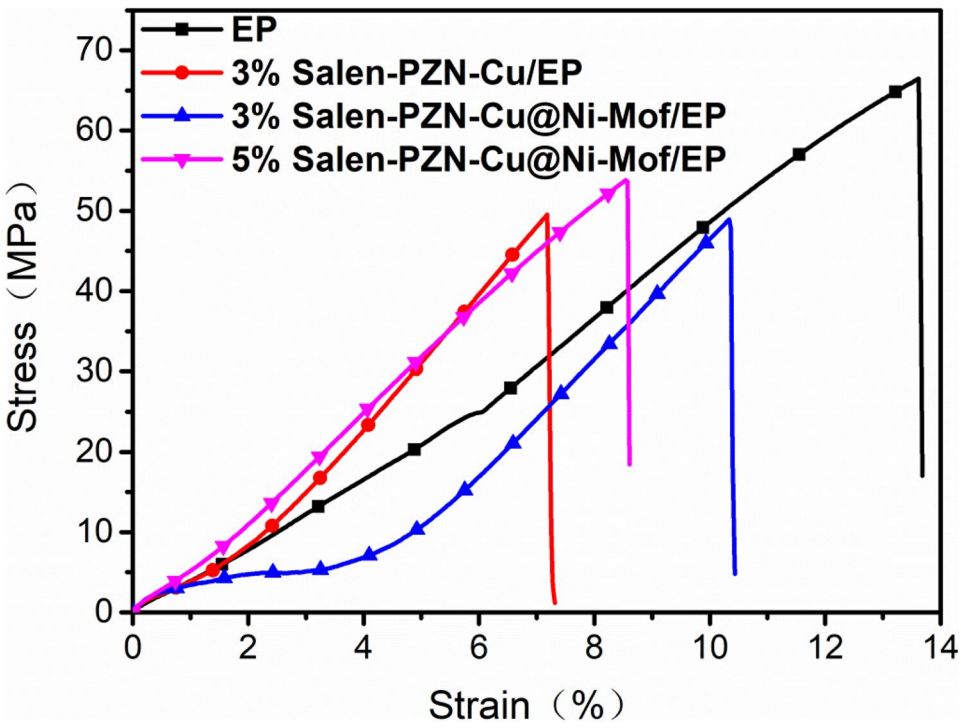

Fig. 11 Stress–strain curves of EP and EP composites

Table 4 Tensile testing results of Salen-PZN-Cu/EP和 Salen-PZN-Cu@Ni-Mof/EP composites

Materials	Tensile strength (MPa)	Young's modolus (MPa)	Strain (%)
EP	66.50	844.08	13.7
3% EP/Salen-PZN-Cu	49.52	725.58	7.32
3% EP/Salen-PZN-Cu@Ni-Mof	48.92	825.80	10.44
5% EP/Salen-PZN-Cu@Ni-Mof	53.84	690.60	8.61

retardant effect [39]. Cu^{2+} ions play a part in catalyzing and changing the cracking process of polymer materials, which catalyzed the formation of CO_2 when the polymer burns to dilute the concentration of flammable gases. In addition, Cu^{2+} ions can catalyze the formation of carbon residue to enhance the flame retardant effect of the condensed phase. Ni-Mof has a strong catalytic effect on carbon formation, the carbon layer as a physical barrier becomes more dense to prevent the escape of degraded volatile products under the co-catalysis of Cu and Ni ions. As a porous material, the organic–inorganic mofs not only improve the compatibility and dispersion between flame retardant and EP, but also absorb toxic smoke such as CO to improve the property of smoke suppression for EP composites. As stated previously, the flame retardant Salen-PZN-Cu@Ni-Mof has an excellent flame retardant effect because of the synergistic effect of Salen-PZN-Cu and Ni-Mof.

Conclusion

A type of novel multifunctional phosphorus-containing organic-inorganic hybrid flame retardant with core-shell structure was prepared and its structure, morphology, composition and thermal stability were characterized by FTIR, SEM, TEM, XPS and TGA. The results showed that the Salen-PZN-Cu@Ni-Mof microspheres with core–shell structure were successfully synthesized. Then Salen-PZN-Cu@Ni-Mof/EP composite was prepared to investigate its thermal stability, flame retardancy, smoke suppression and the mechanism of action on the EP. It turned out that the introduction of Salen-PZN-Cu@Ni-Mof significantly improved the thermal stability of EP composites when the addition amount was 3wt%, the results of the cone calorimeter test showed that adding 3% Salen-PZN-Cu@Ni-Mof made PHRR, THR, SPR and TSP of polymer materials reduced by 30.4%, 10.8%, 29.5% and 6.8%, respectively, showing that Salen-PZN-Cu@Ni-Mof could significantly enhance the fire safety of epoxy resin composites, which was attributed to the synergetic combination of the flame retardant effect of the phosphazene structure itself, the catalyzed carbon formation of various metal ions and the porous mof materials with strong adsorption properties. Besides, it was found that Ni-Mof could strengthen the compatibility between the flame retardant and the EP matrix effectively through the tensile test. The novel core-shell structure of Salen-PZN-Cu@Ni-Mof promised to be a functional filler possesses integrated features of flame retardancy and high ductility.

Supplementary Information The online version contains supplementary material available at https://doi.org/10.1007/s10965-021-02831-4.

Acknowledgements We appreciate the support of the National Nature Science Foundation of China (No. 51465036) and the Development of Science and Technology of Gansu Province(20YF3FA003).

Declarations

Conflict of interest The authors declare that they have no known competing financial interests.

References

1. He WT, Song P, Yu B, Fang Z, Wang H (2020) Flame retardant polymeric nanocomposites through the combination of nanomaterials and conventional flame retardants. Prog Mater Sci 114:100687
2. Seidi F, Movahedifar E, Naderi G, Akbari V, Ducos F, Shamsi R, Vahabi H, Saeb MR (2020) Flame Retardant Polypropylenes: A Review. Polymers 12(8):1701
3. Dasari A, Yu ZZ, Cai GP (2013) Recent developments in the fire retardancy of polymeric materials[J]. Prog Polym Sci 38(9):1357–1387
4. Cheheltani R, Ezzibdeh RM, Chhour P, Kim J, Jurcova M, Hsu JC, Blundell C, Litt HI, Ferrari VA, Allcock HR, Sehgal CM, Cormode DP (2016) Tunable, biodegradable gold nanoparticles as contrast agents for computed tomography and photoacoustic imaging. Biomaterials 102:87–97
5. Fushimi T, Allcock HR (2009) Cyclotriphosphazenes with sulfur-containing side groups: refractive index and optical dispersion. Dalton Trans 14:2477–2481
6. Fushimi T, Allcock HR (2010) Synthesis and optical properties of sulfur-containing monomers and cyclomatrix polyphosphazenes. Dalton Trans 39(22):5349–5355
7. Tataroğlu A, Özen F, Koran K, Dere A, Görgülü AO, Al-Senany N, Al-Ghamdi A, Farooq WA, Yakuphanoglu F (2018) Structural, electrical and photoresponse properties of Si-based diode with organic interfacial layer containing novel cyclotriphosphazene compound. SILICON 10(3):683–691
8. Koran K (2018) Structural, chemical and electrical characterization of organocyclotriphosphazene derivatives and their graphene-based composites. J Mol Struct 1179:224–232
9. Yang ZJ, Zhang W, Wang T, Li JD (2014) Improved thiophene solution selectivity by Cu2+, Pb2+ and Mn2+ ions in pervaporative poly[bis(p-methyl phenyl) phosphazene]desulfurization membrane. J Membrane Sci 454:463–469
10. Yang ZJ, Zhang WY, Li JD, Chen JX (2012) Polyphosphazene membrane for desulfurization: Selecting poly[bis(trifluoroethoxy)

phosphazene] for pervaporative removal of thiophene. Sep Purif Technol 93:15–24
11. Fei ST, Wood RM, Lee DK, Stone DA, Chang HL, Allcock HR (2008) Inorganic-Organic Hybrid Polymers with Pendent Sulfonated Cyclic Phosphazene Side Groups as Potential Proton Conductive Materials for Direct Methanol Fuel Cells. J Membrane Sci 320(1):206–214
12. Liu W, Zheng YL, Li J, Liu L, Huang XB, Zhang JW, Kang XQ, Tang XZ (2012) Novel polyurethane networks based on hybrid inorganic/organic phosphazene-containing nanotubes with surface active hydroxyl groups. Polym Advan Technol 23(1):1–7
13. Ding JH, Wang L, Yu HJ, Yang Q, Deng LB (2008) Progress in Synthesis of Polyphosphazenes. Des Monomers Polym 11(3):215–222
14. Qian LJ, Ye LJ, Qiu Y, Qu SR (2011) Thermal degradation behavior of the compound containing phosphaphenanthrene and phosphazene groups and its flame retardant mechanism on epoxy resin. Polymer 52(24):5486–5493
15. Tao K, Li J, Xu L, Zhao XL, Xue LX, Fan XY, Yan Q (2011) A novel phosphazene cyclomatrix network polymer: Design, synthesis and application in flame retardant polylactide. Polym Degrad Stabil 96(7):1248–1254
16. Zhou X, Qiu SL, Xing WY, Gangireddy CSR, Gui Z, Hu Y (2017) Hierarchical Polyphosphazene@Molybdenum Disulfide Hybrid Structure for Enhancing the Flame Retardancy and Mechanical Property of Epoxy Resins. ACS Appl Mater Inter 9(34):29147–29156
17. Qiu SL, Xing WY, Mu XW, Feng XM, Ma C, Yuen RK, Hu Y (2016) A 3D Nanostructure Based on Transition-Metal Phosphide Decorated Heteroatom-Doped Mesoporous Nanospheres Interconnected with Graphene: Synthesis and Applications. ACS Appl Mater Inter 8(47):32528–32540
18. Heydari-Bafrooei E, Amini M, Ardakani MH (2016) An electrochemical aptasensor based on TiO2/MWCNT and a novel synthesized Schiff base nanocomposite for the ultrasensitive detection of thrombin. Biosens Bioelectro 85:828–836
19. Feng XR, Li D, Han JD, Zhuang XL, Ding JX (2017) Schiff base bond-linked polysaccharide-doxorubicin conjugate for upregulated cancer therapy. Mat Sci Eng C 76:1121–1128
20. Jeevadason AW, Murugavel KK, Neelakantan MA (2014) Review on Schiff bases and their metal complexes as organic photovoltaic materials. Renew Sust Energ Rev 36:220–227
21. Manjunatha KB, Rajarao R, Umesh G, Bhat BR, Poornesh P (2017) All-optical switching and limiting properties of a Ru (II) Schiff-base complex for nonlinear optical applications. Laser Phys 27(8):85401
22. Rhodes J, Chen H, Hall SR, Beesley JE, Jenkins DC, Collins P, Zheng B (1995) Therapeutic potentiation of the immune system by costimulatory Schiff-base-forming drugs. Nature 377(6544):71–75
23. Su HY, Zhang W, Wu YY, Han XD, Liu G, Jia QM, Shan XY (2018) Schiff base-containing dextran nanogel as pH-sensitive drug delivery system of doxorubicin: Synthesis and characterization. J Biomater Appl 33:088532821878396
24. Seifzadeh D, Valizadeh-Pashabeigh V, Bezaatpour A (2016) 5-CM-Salophen schiff base as an effective inhibitor for corrosion of mild steel in 0.5 M HCl. Chem Eng Commun 203(10):1279–1287
25. El-Lateef HMA, Ismael M, Mohamed IMA (2015) Novel Schiff base amino acid as corrosion inhibitors for carbon steel in CO2-saturated 3.5% NaCl solution: experimental and computational study. Corros Rev 33:77–97
26. Naik A, Bourbigot S, Bellayer S, Touati N, Tayeb KB, Vezin H, Fontaine G (2018) Salen complexes as fire protective agents for thermoplastic polyurethane: Deep electron paramagnetic resonance spectroscopy investigation. ACS Appl Mater Inter 10(29):24860–24875
27. Wei WC, Deng C, Huang SC, Wei YX, Wang YZ (2018) Nickel-Schiff base decorated graphene for simultaneously enhancing the electroconductivity, fire resistance, and mechanical properties of a polyurethane elastomer. J Mater Chem 6(18):8643–8654
28. Ramgobin A, Fontaine G, Penverne C, Bourbigot S (2017) Thermal stability and fire properties of salen and metallosalens as fire retardants in thermoplastic polyurethane (TPU). Materials 10(6):665
29. Xu GJ, Meng ZS, Guo XJ, Zhu HW, Deng KM, Xiao CY, Liu YZ (2019) Molecular simulations on CO2 adsorption and adsorptive separation in fullerene impregnated MOF-177, MOF-180 and MOF-200. Comp Mater Sci 168:58–64
30. Ha NT, Lefedova OV, Ha NN (2016) Theoretical study on the adsorption of carbon dioxide on individual and alkali-metal doped MOF-5s. Russ J Phys Chem A+ 90(1):220–225
31. Kadioglu O, Keskin S (2018) Efficient separation of helium from methane using MOF membranes. Sep Purif Technol 191:192–199
32. Ke F, Qiu LG, Yuan YP, Jiang X, Zhu JF (2012) Fe3O4@MOF core–shell magnetic microspheres with a designable metal–organic framework shell. J Mater Chem 22(19):9497–9500
33. Lee J, Farha OK, Roberts J, Scheidt KA, Nguyen ST, Hupp JT (2009) Metal–organic framework materials as catalysts. Chem Soc Rev 38(5):1450–1459
34. Hou YB, Liu LX, Qiu SL, Zhou X, Gui Z, Hu Y (2018) DOPO-modified two-dimensional co-based metal-organic framework: Preparation and application for enhancing fire safety of poly(lactic acid). ACS Appl Mater Inter 10(9):8274–8286
35. Cui JF, Zhang YB, Wang LR, Liu H, Wang NN, Yang BP, Guo JH, Tian L (2020) Phosphorus-containing Salen-Ni metal complexes enhancing the flame retardancy and smoke suppression of epoxy resin composites. J Appl Polym Sci 137(21):48734
36. Hou YB, Hu WZ, Gui Z, Hu Y (2017) Preparation of metal-organic frameworks and their application as flame retardants for polystyrene. Ind Eng Chem Res 56:8
37. Sun XJ, Wu TT, Yan ZM, ChenWJ LXB, Xia QB, Chen SY, Wu QH (2019) Novel MOF-5 derived porous carbons as excellent adsorption materials for n-hexane. J Solid State Chem 271:354–360
38. Zhao L, Zhao CX, Guo CY, Li YT, Li SL, Sun LY, Li H, Xiang D (2019) Polybenzoxazine resins with polyphosphazene microspheres: synthesis, flame retardancy, mechanisms, and applications. ACS Omega 4(23):20275–20284
39. Naik AD, Fontaine G, Bellayer S, Bourbigot S (2015) Crossing the traditional boundaries:salen-based Schiff bases for thermal protective applications. ACS Appl Mater Inter 7(38):21208–21217